

Diffraction Radiation of Electron Beam in the Presence of Dielectric Optical Nanowire Resonator

Dariia O. Yevtushenko,^{1,2} Alexander. I. Nosich,² Sergii V. Dukhopelnykov,^{2,3} Eugene N. Odarenko¹

¹Department of Photonics and Laser Engineering, Kharkiv National University of Radio Electronics, Kharkiv 61066, Ukraine

²Laboratory of Micro and Nano Optics, Institute of Radio-Physics and Electronics NASU, Kharkiv 61085, Ukraine

³Department of Mathematics, National Technical University “Kharkiv Polytechnic Institute,” Kharkiv 61002, Ukraine

dariia.yevtushenko@gmail.com

Abstract—The optical diffraction radiation that accompanies the motion of a modulated beam of electrons near a dielectric nanowire scatterer is investigated in the two-dimensional formulation. Our goal is to compute the field in the near and far zones and analyze how it depends on electron beam parameters. We demonstrate the excitation of internal resonances of such a scatterer that can be useful in the design of nanoscale non-invasive beam position monitors.

Index Terms— diffraction radiation; nanowire scatterers; Smith-Purcell effect; surface wave; total scattering cross-section

I. INTRODUCTION

Radiation of electrons passing in the vicinity of a periodic structure made of some conducting material is called the Smith-Purcell effect (SPE) [1]. It has been studied by both experimentalists and theoreticians for over 60 years now since its discovery [2-5]. Today, SPE is viewed as the most practically important however still particular case of more broadly defined effect: the radiation of the surface and polarization currents induced on various material objects in various frequency regions by the charged particles or their beams, which do not touch or hit these material objects. To distinguish this type of electromagnetic-wave radiation from the others, such as, for instance, the transient radiation, it is commonly called the *diffraction radiation* (DR) [3-10].

Detection of DR in the visible wavelength region, called the optical DR is the most promising technique for application to noninvasive beam diagnostics [6-10]. Here, the emergence and rapid development of nanotechnologies opens the way to use nanoscale scatterers and associated resonances on the surface-plasmonic and dielectric modes as sensitive antennas [11,12]. Indeed, such antennas radiate the optical waves, characterized with the far-field patterns and the carried power values depending on the electron-beam bunching, velocity, and fine distance to the beam trajectory. For instance, for the configuration in Fig. 1, the measurement of the DR pattern can deliver the information on the beam position shift h and velocity v .

Note that the nanowires can be designed resonant and, moreover, tunable by covering the wires with the graphene [13-15]. Nanoscale size of such beam-sensor antennas introduces negligible distortion to the beam energy characteristics, which

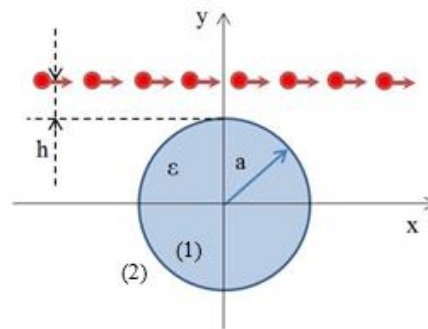


Fig. 1. Cross-sectional geometry of an electron beam moving near a circular dielectric nanowire.

can be considered as fixed. This makes possible the analysis of sensing antenna elements in the same way as within the traditional antenna theory, i.e. as the scattering of the given electromagnetic field of the moving beam by the conducting and dielectric scatterers of given shapes and material properties. The latter parameters can be manipulated to optimize the beam-diagnostics antenna performance.

II. SCATTERING CONFIGURATION AND BEAM FIELD

We assume that two-dimensional (2-D) electron beam with the harmonic time dependence $e^{-i\omega t}$ is moving over a circular dielectric nanowire with radius a , and dielectric permeability ε at the distance h from it's surface. Hence, the beam distance from the x -axis is $p = h + a$. Besides, we denote the inner and the outer domains of the wire as domains (1) and (2), respectively, and introduce the Cartesian and the polar coordinates as shown in Fig. 1.

Consider the diffraction radiation, which accompanies a uniform motion of a plane unbounded electron beam moving along the straight trajectory with velocity $v = \beta c$ ($\beta < 1$) near the dielectric wire. The charge density function is then given by

$$\rho = \rho_0 \delta(y - p) \exp[i(kx / \beta - \omega t)], \quad (1)$$

where $\delta(\cdot)$ is the Dirac delta function, ω and ρ_0 are the frequency and the amplitude of beam modulation, $k = \omega / c$ is the free-space wavenumber, and c is the light velocity.

We will consider the electromagnetic-field problem in the given-current approximation. In this case the incident wave is

the field of the sheet current beam (1) moving in the free space. As it was shown in [2], this field has the form of a slow inhomogeneous plane wave of the surface nature, the only nonzero component of the magnetic field of which is

$$H_z(x, y) = A \text{sign}(y-p) e^{-q|y-p|} e^{i(k/\beta)x} \quad (2)$$

where $q = k\gamma/\beta$, $\gamma = (1-\beta^2)^{1/2}$, function $\text{sign}(y-p)$ is the sign of the expression in the brackets, time dependence is omitted, and $A > 0$ is a constant. This is a surface wave running along the beam trajectory in the positive direction of the x -axis. Note that the modulation of the electron beam can be achieved by its preliminary bunching in periodic waveguide or through direct modulation by a laser emission [6,12].

III. PROBLEM FORMULATION

In the presence of the scatterer, the total field in the external medium is characterized by the sum $H_z^{\text{tot}} = H_z^{\text{in}} + H_z^{(2)}$.

In addition, in the scatterer the field $H_z^{(1)}$ is different from (2).

The unknown field function must satisfy the conditions:

1. The Helmholtz equation with coefficient $k_1 = \alpha k$ in domain (1) and $k_2 = k = \omega/c$ in domain (2),

$$(\Delta + k_{1,2}^2) H^{(1,2)}(\vec{r}) = 0 \quad (3)$$

2. The boundary conditions at $r = a$ and $0 \leq \varphi < 2\pi$,

$$H^{(1)} = H^{\text{in}} + H^{(2)}, \quad E_\varphi^{(1)} = E_\varphi^{\text{in}} + E_\varphi^{(2)}; \quad (4)$$

note that from Maxwell's equations it follows that

$$E_\varphi^{(1,2)} = Z_0 (ik\epsilon_{1,2})^{-1} \partial H_z^{(1,2)} / \partial r, \quad (5)$$

where the polar coordinates (r, φ) relate to the Cartesian ones as $x, y = r(\cos, \sin)\varphi$ and $Z_0 = (\mu_0/\epsilon_0)^{1/2}$ is vacuum impedance,

3. The condition for the local power finiteness,
4. The radiation condition at infinity (outgoing wave behavior),

$$H^{(2)}(r, \varphi) \square 2^{1/2} (i\pi k_2 r)^{-1/2} e^{ik_2 r} \Phi(\varphi) \text{ at } r \rightarrow \infty, \quad (6)$$

These conditions guarantee the solution uniqueness.

IV. BASIC EQUATIONS

The circular shape of the boundaries between different materials suggests the use of the method of separation of variables. This means we expand the field functions in each domain in terms of Fourier series in the angular coordinate φ , in particular, if $r \sin \varphi < p$ and $r > a$ then

$$H_z^{\text{in}}(\vec{r}) = -Ae^{-q\rho} e^{ikr \cos(\varphi+\psi)}, \quad (7)$$

where we introduce the complex incidence angle ψ , such that

$$\cos \psi = 1/\beta, \quad \sin \psi = i\gamma/\beta, \quad (8)$$

and, according to the Anger formula, obtain

$$H^{\text{in}}(\vec{r}) = -Ae^{-q(h+a)} \sum_{m=-\infty}^{+\infty} i^m J_m(kr) (1-\gamma)^m \beta^{-m} e^{im\varphi} \quad (9)$$

The scattered field is expressed as

$$H^{\text{sc}}(\vec{r}) = \sum_{m=-\infty}^{+\infty} \begin{cases} a_m J_m(k_1 r), & r < a \\ b_m H_m^{(1)}(kr), & r > a \end{cases} e^{im\varphi}, \quad (10)$$

where a_m, b_m are unknown coefficients and J_m and $H_m^{(1)}$ are the Bessel and Hankel (first kind) functions. The coefficients

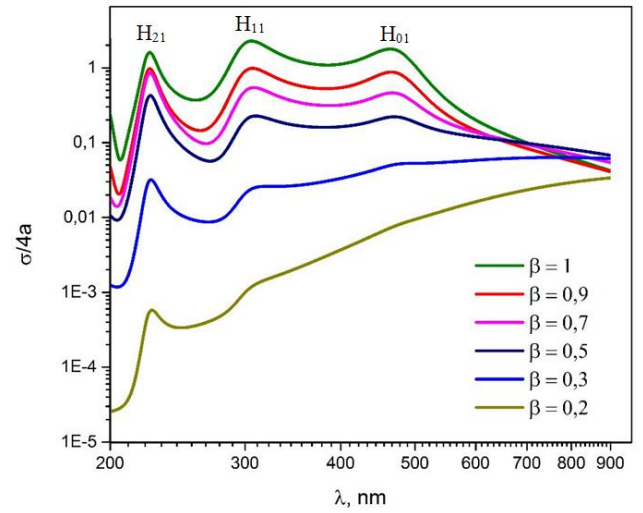


Fig. 2. Normalized TSCS of the 50-nm in radius lossless silicon nanowire ($\epsilon = 12$) versus the wavelength in the visible range, for several values of the electrons' relative velocity β . Note the resonances on the wire modes.

are found using the conditions 1. to 4. in analytical form as

$$a_m = C [f_m(ka) H'_m(ka) - H_m(ka) f'_m(ka)] (\Delta_m)^{-1}, \quad (11)$$

$$b_m = C [f_m(ka) \alpha J'_m(k\alpha a) - J_m(k\alpha a) f'_m(ka)] (\Delta_m)^{-1}, \quad (12)$$

where the superscripts of the Hankel functions and their derivatives are omitted, and other notations are

$$C = -Ae^{-q(h+a)}, \quad (13)$$

$$f_m = i^m J_m(ka) (1-\gamma)^m \beta^{-m}, \quad f'_m = i^m J'_m(ka) (1-\gamma)^m \beta^{-m}, \quad (14)$$

$$\Delta_m = J_m(k\alpha a) H'_m(ka) - \alpha J'_m(k\alpha a) H_m(ka), \quad (15)$$

Here, characteristic equations of the considered scatterer,

$$\Delta_m(k) = 0, \quad m = 0, \pm 1, \pm 2, \dots, \quad (16)$$

may have only complex solutions, k_{mm} , which form a discrete set with negative imaginary parts. These are complex natural wavenumbers of the modes of dielectric wire as open cavity, usually denoted as $H_{m,n}$ where $m = 0, 1, \dots$ and $n = 1, 2, \dots$.

The scatterer will be characterized with its total scattering cross-sections (TSCS),

$$\sigma_{sc} = \frac{4}{kA^2} \sum_{m=-\infty}^{+\infty} |b_m|^2, \quad (17)$$

which is the result of integration of the Poynting vector flux of the scattered field over all space directions. Presented further results for quantities (17) are normalized by $4a$ that is the limit value of σ_{sc} at $\beta = 1$ and $a/\lambda \rightarrow \infty$.

V. NUMERICAL RESULTS

We have studied the DR characteristics for the scatterer shaped as a circular dielectric wire shown in Fig. 1.

The plots in Fig. 2 demonstrate the dependences of the normalized TSCS on the modulation wavelength in the visible range, for the wire with the radius 50 nm, relative dielectric constant $\epsilon = 12$, the separation distance $h = 10$ nm, and several values of the relative beam velocity β . As one can see, due to rather high optical contrast of silicon, even such a tiny wire behaves as an open nanocavity.

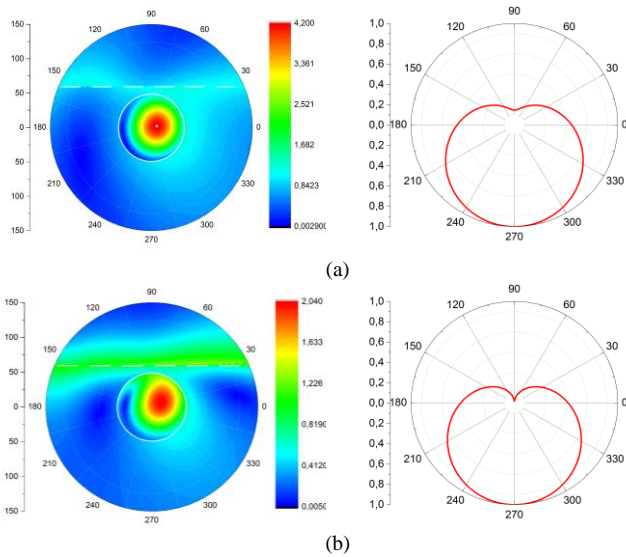


Fig. 3. Near magnetic field patterns (left) and normalized far-field scattering pattern (right) of the lossless silicon nanowire of the radius $a = 50$ nm for $\lambda = 464$ nm and $\beta = 0.8$ (a), $\beta = 0.5$ (b) in the resonance on the mode H_{01} .

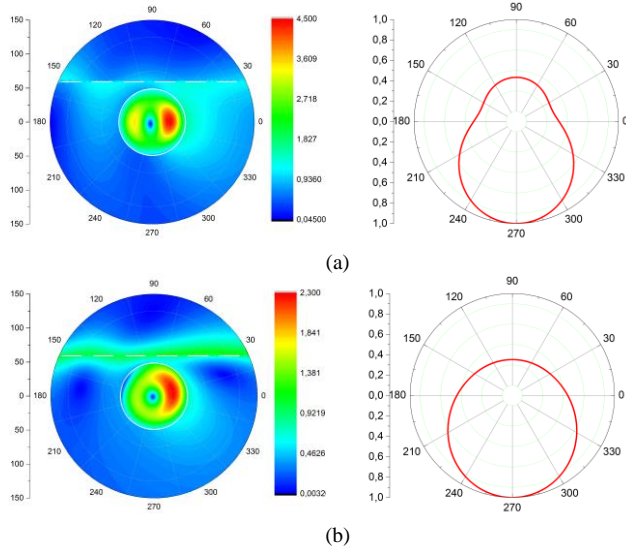


Fig. 4. The same as in Fig. 3 however for the mode H_{11} at $\lambda = 306$ nm.

Indeed, for all values of the relative beam velocity β the spectra of TSCS display three distinctive peaks in the visible and ultra-violet ranges. Their wavelengths positions at 464 nm, 306 nm, and 225 nm do not depend on the relative beam velocity β .

The panels of Figs. 3 to 5 show the in-resonance near field patterns for the same dielectric nanowire as in Fig. 2 and two values of β . One can clearly see the straight trajectory of the beam at the distance $h = 10$ nm above the wire. The bright spots of the field inside the wire enable one to identify the resonating modes. The lowest of them, in frequency, is the H_{01} mode at 464 nm that is certified by the single bright spot near to wire's center. The next, in frequency, is the dipole mode H_{11} at 306 nm showing two bright spots. The most high-frequency peak at 225 nm is on the quadrupole mode H_{21} . This field pattern is well visible for the relativistic beam DR, as at $1 - \beta \ll 1$ the beam field (2) is very close to a plane wave,

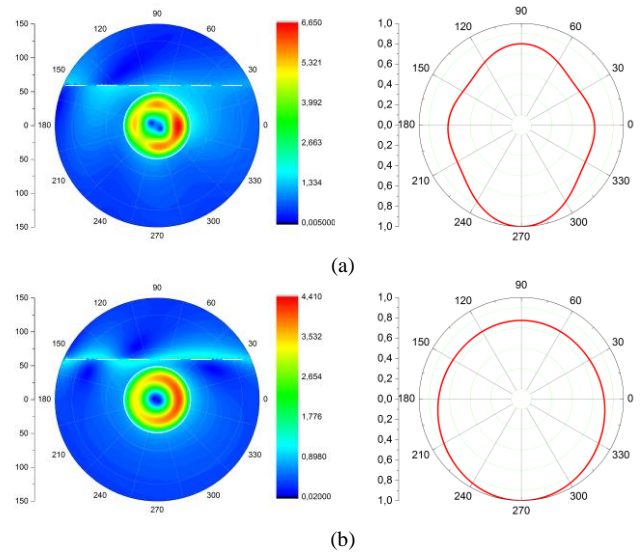


Fig. 5. The same as in Figs. 3 and 4 however for the mode H_{21} at $\lambda = 225$ nm.

albeit with a jump at the beam trajectory.

Here, it is necessary to remind that if $\beta \neq 0$ the incident field (2) is not symmetric with respect to the wire section by the x -axis. Therefore, at the resonance wavelengths, the beam field excites not a single one of two degenerate wire modes $H_{m,n}$ ($m > 0$) but the both, and the contribution of the anti-symmetric with respect to $y = 0$ component gets larger with smaller β . This leads to the overlap of two modal patterns so that the resulting field portrait resembles a continuous ring. The reason is that if $\beta \ll 1$ (non-relativistic beam) then the contributions of both components to the resonance field differ only by the factor (i). Hence the inner field pattern becomes the clockwise rotating wave, $J_m(k\alpha a)(\cos m\varphi + i \sin m\varphi) + O(\beta)$, instead of the standing-wave $J_m(k\alpha a)\cos m\varphi$, observed in the plane wave scattering.

This feature is also well visible in the far zone, where the normalized by maximum value angular scattering patterns are also shown in Figs. 3 to 5 at the same wavelengths. If $\beta \ll 1$, then the in-resonance radiation becomes omnidirectional. Note that this is not true for the resonance on the H_{01} mode (Fig. 3) because in this case the contribution of anti-symmetric field component is close to zero.

VI. CONCLUSIONS

If one can neglect the action of the field on the electrons, then the electromagnetic field of a modulated 2-D beam takes form of a surface wave propagating along the beam trajectory. This wave induces the polarization and surface currents on the local obstacles and hence a radiation occurs even if the beam does not touch the obstacle. In fact, the wire plays the role of optical nanoantenna, which makes the beam of particles visible. As we have shown, a nanowire behaves as an open resonator, thanks to which the radiated power is enhanced near the natural-mode wavelengths. Unlike the more conventional plane-wave scattering, the in-resonance fields (except of the resonance on the H_{01} mode) are shaped as rotating cylindrical waves. This happens because of three circumstances: (i) the

beam field depends on y , and hence there are no “dark modes” of the wire that remain not excited because of orthogonal symmetry with respect to the incident wave, (ii) the symmetric and the anti-symmetric natural modes of the wire remain degenerate, and (iii) if $\beta \rightarrow 0$, then the phase shift between two field components becomes $\pi/2$.

REFERENCES

- [1] S. J. Smith and E. M. Purcell, “Visible light from localized surface charges moving across a grating,” *Phys. Rev.*, vol. 92, art. 1069, 1953.
- [2] P. M. van den Berg, “Smith-Purcell radiation from a line charge moving parallel to a reflection grating,” *J. Opt. Soc. Am.*, vol. 63, no 6, pp. 689-698, 1973.
- [3] A. I. Nosich, “Diffraction radiation which accompanies the motion of charged particles near an open resonator,” *Radiophysics Quant. Electron.*, vol. 24, no 8, pp. 696-701, 1981.
- [4] M. Castellano, “A new non-intercepting beam size diagnostics using diffraction radiation from a slit,” vol. 394, pp. 275-280, 1997.
- [5] A. P. Potylitsyn, “Resonant diffraction radiation and Smith-Purcell effect,” *Phys. Lett. A*, vol. 238, pp. 112-116, 1998.
- [6] M. Castellano, *et al.*, “Measurements of coherent diffraction radiation and its application for bunch length diagnostics in particle accelerators,” *Phys. Rev. E*, vol. 63, art. no 056501, 2001.
- [7] P. Karataev, S. Araki, R. Hamatsu, *et al.*, “Beam-size measurement with optical diffraction radiation at KEK accelerator test facility,” *Phys. Rev. Lett.*, vol. 93, art. no 244802, 2004.
- [8] Y. A. Goponov, R. A. Shatokhin, and K. Sumitani, “Diffracted diffraction radiation and its application to beam diagnostics,” *Nuclear Instrum. Meth. A*, vol. 885, pp. 134-138, 2018.
- [9] L. Bobb, R. Kieffer, *et al.*, “Feasibility of diffraction radiation for noninvasive beam diagnostics as characterized in a storage ring,” *Phys. Rev. Accel. Beams*, vol. 21, art. no 03801, 2018.
- [10] T. Muto, S. Araki, *et al.*, “Observation of incoherent diffraction radiation from a single-edge target in the visible-light region,” *Phys. Rev. Lett.*, vol. 90, no 10, pp. 104801-104804, 2003.
- [11] N. Talebi, “Interaction of electron beams with optical nanostructures and metamaterials: from coherent photon sources towards shaping the wave function,” *J. Opt.*, vol. 19, art. no 103001, 2017.
- [12] K. J. Leedle, A. Ceballos, H. Deng, *et al.*, “Dielectric laser acceleration of sub-100 keV electrons with silicon dual-pillar grating structures,” *Opt. Lett.*, vol. 40, no, 18, pp. 4344-4347, 2015.
- [13] M. Riso, M. Cuevas and R. A. Depine, “Tunable plasmonic enhancement of light scattering and absorption in graphene-coated subwavelength wires,” *J. Opt.*, vol. 17, pp. 075001/8, 2015.
- [14] M. Cuevas, *et al.*, “Complex frequencies and field distributions of localized surface plasmon modes in graphene-coated subwavelength wires,” *J. Quant. Spect. Rad. Transfer*, vol. 173, pp. 26-33, 2016.
- [15] M. Naserpour, C. J. Zapata-Rodriguez, S. M. Vuković, *et al.*, “Tunable invisibility cloaking by using isolated graphene-coated nanowires and dimers,” *Sci. Rep.*, vol. 12, pp. 12186/14, 2017.